International Journal of Engineering and Technology Volume 2 No. 12, December, 2012

Modeling of Wind Turbines Equipped with Induction Machines for Voltage Profile Studies Using PSCAD

T. Abedinzadeh, J.Pouladi
Islamic Azad University, Shabestar Branch, Shabestar, Iran

ABSTRACT

As a result of increasing environmental concern, more and more electricity is generated from wind turbines. Therefore, adequate models to study the impact of wind turbines on electrical power system behavior are needed**.** One of the most important considerations is the effect of wind turbines on the voltage profile, i.e. the induced slow voltage variations, which are the subject of this paper. The wind turbines can be operated in two modes: constant-speed and variable-speed. Each one of these cases has different impact on steady state voltage of distribution grids. For evaluation of these impacts, SCIG generator has been simulated that works in constant-speed operation and DFIG generator that is used in a variable-speed turbine. Variable-speed wind turbines can be controlled in two ways. They can produce power with constant power factor or they control magnitude of voltage of PCC. PSCAD/EMTDC simulation program is used to investigate the impact of these turbines on a distribution grid. The outcomes of the simulation demonstrate the effectiveness of the proposed simulation and control schemes. Also, it is shown that voltage control scheme has better results and improves the voltage profile considerably.

Keywords: *Wind turbine, Voltage profile, DFIG, SCIG, Vector control, PSCAD/EMTDC*

1. INTRODUCTION

Wind energy is said to be one of the most prominent sources of electrical energy in years to come. Wind energy conversion systems (WECS) are the devices which are used to convert wind energy to electrical energy. The increasing concerns to environmental issues demand the search for more sustainable electrical sources [1-5]. With the wind farms rating hundreds megawatts, the concerns start to focus on the voltage problems of the power system [6]. For distribution grids connected wind power generation, voltage quality is an important issue for the system planning purpose. The operation of wind turbines in the distribution networks may affect the voltage quality offered to the consumers.

Most of the models used to represent a wind turbine are based on a non linear relationship between rotor power coefficient and linear tip speed of the rotor blade [5, 7-9].

On the dynamic subject, several works have been done on the analysis of power quality from wind turbines to the power systems [6, 10-13]. An extensive analysis of the potential impacts of wind turbines has been developed on the power quality, where the work focused on the small scale integration and is explained how to assess the voltage quality from wind turbines using wind turbine characteristics.

The turbine of wind energy conversion systems can he operated in one of two modes: constant-speed and variable-speed. In constant-speed turbines, reactive power cannot be controlled.

But reactive power of variable-speed turbines can be controlled in two ways. They can produce power with constant power coefficient or they can be controlled to adjust magnitude of voltage of PCC (Point of Common Coupling). Presently, the trend of operating wind turbines is in the variable-speed mode. One of the most common type of wind turbines is the variable speed wind turbines with Doubly-Fed Induction Generator (DFIG). In the DFIG, the applied rotor voltage controls the real and reactive powers and generator's speed, when its stator terminals are connected to a power system and the stator voltage is held constant by the grid[2, 3, 5, 12-16].

Each one of these cases has different impact on steady state voltage of distribution grids. For evaluation of these impacts, SCIG (Squirrel Cage Induction Generator) that works in constant-speed operation and DFIG generator that is used in a variable-speed turbine have been simulated. A simulation program of PSCAD/EMTDC is used to investigate the impact of these turbines on a distribution grid. Both of above-mentioned methods are applied under same disturbances in wind speed in the simulation. This simulation is based on a vector control of the DFIG machine. The technique of vector control is used to control the output parameters of the rotor in different loading conditions and variable rotor speeds [9, 17, 18].

2. WIND TURBINE

Wind energy conversion systems (WECS) are the devices which are used to convert the wind energy to electrical energy. The total wind power entering the wind turbine is given by:

$$P_T = \frac{1}{2}\rho A V^3 C_p \quad (1)$$

Where ρ is the density of air in kg/m^3 and A is the area swept by the blades of wind turbine, in m^2 and V is the speed of wind in m/s and C_P is dimensionless power coefficient.

Since calculation of C_P is too complicated, usually its value is calculated by recourse to simpler formulas. The formula used for C_P is [9]:

$$C_p = (0.44 - 0.0167\beta)Sin\left(\frac{\pi(\lambda - c_1)}{c_2 - 0.3\beta}\right) - 0.00184(\lambda - c_1)\beta \quad (2)$$

Where λ is Tip-Speed Ratio (TSR) and β is the blade pitch angle. C_1 and C_2 are two coefficients that equal 1 and 18, respectively.

The TSR dictates the operating condition of a turbine. A typical power coefficient C_P versus TSR is given in Fig. 1. As the wind speed changes, the Tip-Speed Ratio and C_P will vary. The C_P characteristic has single maximum at a specific value of TSR. Therefore if the wind turbine is operating at constant speed then the power coefficient will be maximum only at one wind speed.

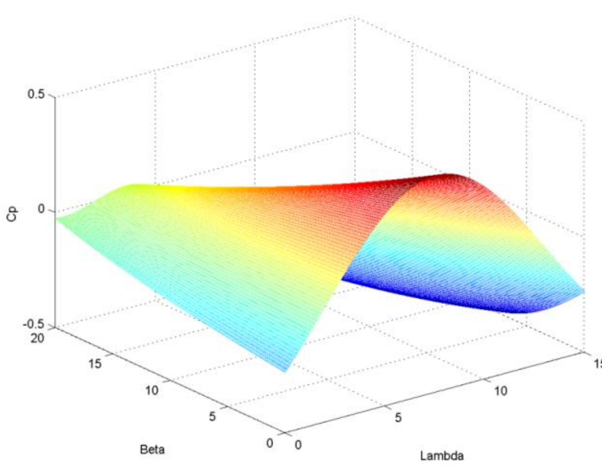

Fig. 1 Typical C_P versus TSR

In a wind power system typically the wind turbine starts operating (cut-in speed) when the wind speed exceeds 3-4m/s, and is shut off at speeds exceeding 25 to 30m/s. In between, it can operate in the optimum constant C_P region, the speed-limited region or the power-limited region as shown in Fig. 2. Optimum power extractor makes turbine to work in these regions.

2.1 Pitch Angle

The block diagram that is used to control pitch angle is shown in Fig .2.

This controller increase pitch angle if turbine shaft speed exceeds its maximum speed. But pitch angle can only rise some degrees (here 20 degrees).

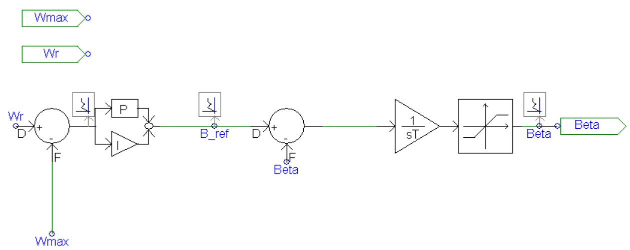

Fig. 2 Pitch angle control block diagram

2.2 Optimum Power Extractor

This section dictates turbine operating conditions and specifies optimum C_P to obtain reference torque and reference speed of generator. On the other hand, if turbine power exceeds its maximum value, Optimum Power Extractor should control it with varying C_P.

2.3 Turbine Simulation

Below equation is used for turbine simulation:

$$T_T = \frac{P_T}{\omega_r} = \frac{\rho\pi D_T^2 V_w^3 C_p}{2\omega_r} \quad (3)$$

Where ρ = 1.225 and turbine blade radius is 23 m. V_w is wind speed and is turbine shaft speed.

3. DFIG GENERATOR

A double-Fed induction generator is, in fact, a standard wound rotor induction generator with its stator windings directly connected to the power grid and rotor connected to the power grid through a frequency converter (Fig.3) [17].

So it delivers power from stator to the grid. The rotor, depending on its voltage, can either deliver power to the grid or absorb it.

ISSN: 2049-3444

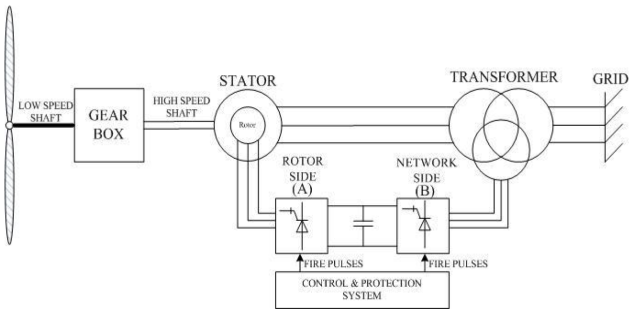

Fig.3 DFIG overall system in a wind turbine-generator

In modern DFIG designs, the frequency converters are usually built by two, three phase self commutated back-to-back PWM converters with an intermediate capacitor link for DC bus voltage regularity. The converter that is connected to the rotor called 'rotor side converter' and the other named 'grid side converter'. By controlling the grid and rotor converters, the DFIG can be adjusted to achieve many capabilities versus conventional squirrel cage induction generators.

The dq representation of DFIG machine are given by[7]:

For the stator side:

$$\lambda_{ds} = -L_s i_{ds} + L_m i_{dr} \quad (4)$$

$$\lambda_{qs} = -L_s i_{qs} + L_m i_{qr} \quad (5)$$

$$v_{ds} = -R_s i_{ds} - \omega_s \lambda_{qs} + \frac{d\lambda_{ds}}{dt} \quad (6)$$

$$v_{qs} = -R_s i_{qs} + \omega_s \lambda_{ds} + \frac{d\lambda_{qs}}{dt} \quad (7)$$

For the rotor side:

$$\lambda_{dr} = L_r i_{dr} - L_m i_{ds} \quad (8)$$

$$\lambda_{qr} = L_r i_{qr} - L_m i_{qs} \quad (9)$$

$$v_{dr} = R_r i_{dr} - s\omega_s \lambda_{qr} + \frac{d\lambda_{dr}}{dt} \quad (10)$$

$$v_{qr} = R_r i_{qr} + s\omega_s \lambda_{dr} + \frac{d\lambda_{qr}}{dt} \quad (11)$$

The electrical output power from the induction generator is given by:

$$P_s = \frac{3}{2}(v_{ds} i_{ds} + v_{qs} i_{qs}) \quad (12)$$

$$P_r = \frac{3}{2}(v_{dr} i_{dr} + v_{qr} i_{qr}) \quad (13)$$

$$P_g = P_s - P_r \quad (14)$$

Where P_s is the power delivered by the stator, P_r is the power to the rotor, P_g is the total power generated and delivered to the grid.

And reactive power:

$$Q_s = \frac{3}{2}(v_{qs} i_{ds} - v_{ds} i_{qs}) \quad (15)$$

The electrical torque generated by induction machine is given by:

$$T_e = -\frac{3}{2} P(\lambda_{ds} i_{qs} - \lambda_{qs} i_{ds}) \quad (16)$$

And the mechanical equation for machine is:

$$T_m - T_e = J\frac{d\omega_r}{dt} + D\omega_r \quad (17)$$

Where T_m is mechanical torque and T_e is electromagnetic torque in Nm, is mechanical shaft speed in rad/sec, D is fiction coefficient in Nm/rad/s and J is inertia in kg-m^2.

In this paper, the power converter that is between grid and rotor is considered ideal.

4. VECTOR CONTROL

The technique of vector control will be used in the control of induction generator to control the generated voltage for different loading conditions and variable rotor speeds. The total stator flux is aligned along the d-axis of the rotating reference frame so that [7]: $\lambda_{qs} = 0$

So i_{qs} is derived:

$$i_{qs} = -\frac{L_m}{L_{ls} + L_m} i_{qr} \quad (18)$$

Substituting iqs in (9), (10) will result in:

$$v_{dr} = R_r i_{dr} - s\omega_s\left(\left(L_r - \frac{L_m^2}{L_s}\right) i_{qr}\right) + \left(L_r - \frac{L_m^2}{L_s}\right)\frac{d}{dt} i_{dr} \quad (19)$$

$$v_{qr} = R_r i_{qr} + s\omega_s\left(\left(L_r - \frac{L_m^2}{L_s}\right) i_{dr} + \left(\frac{L_m V_s}{L_s \omega_s}\right)\right) + \left(L_r - \frac{L_m^2}{L_s}\right)\frac{d}{dt} i_{qr} \quad (20)$$

$$T_e = -\frac{3}{2}P\frac{L_m}{L_{ls}+L_m}\lambda_{ds}i_{qr} \quad (21)$$

Neglecting stator resistance will lead to[7]:

$$V_{ds} = 0 \quad (22)$$

$$V_{qs} = \omega_s \lambda_{ds} \quad (23)$$

Substituting for V_{ds}=0 ,(11) and (12) will be simplified as follows:

$$P = \frac{3}{2}(v_{qs}i_{qs}) \quad (24)$$

$$Q = \frac{3}{2}(v_{qs}i_{ds}) \quad (25)$$

4.1 Electromagnetic Torque/Speed Control

Optimum Power Extractor calculates desired torque for turbine. Therefore, i_{qrref} will be derived as shown in Fig.4 (a). Comparing the reference variable to the actual machine current, an error signal required for controlling the speed of the machine is obtained. To determine the required rotor voltage, a standard PI controller and the summation of the direct rotor current compensation term, derived from (20), is implemented. This control scheme is shown in Fig. 4(b).

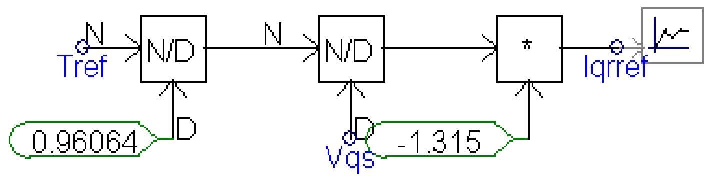

a) Primary stage

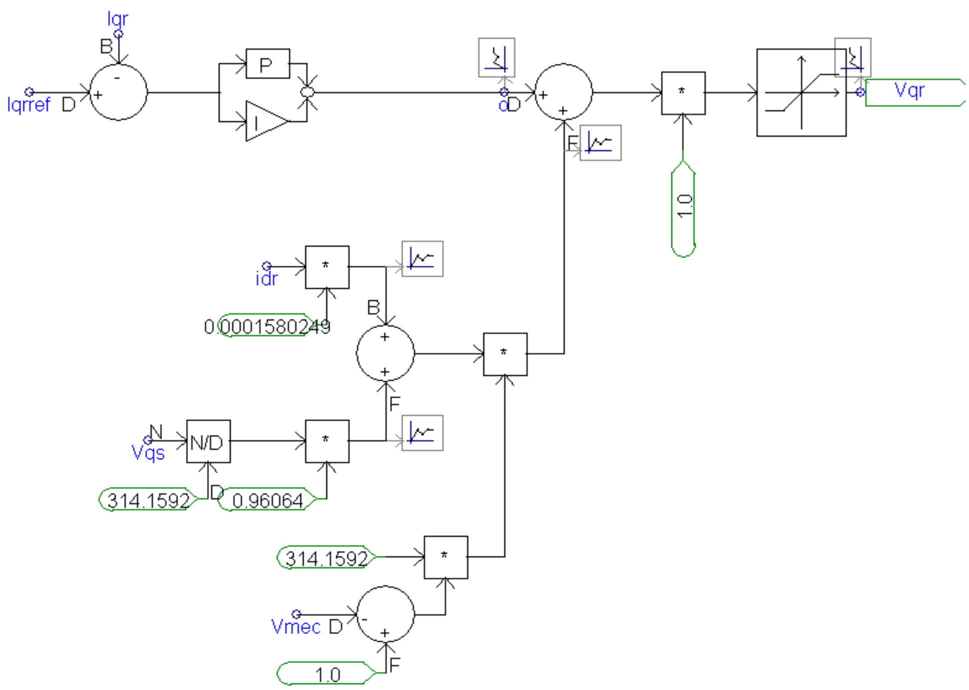

b) Secondary stage

Fig. 4 Speed control scheme based on vector control

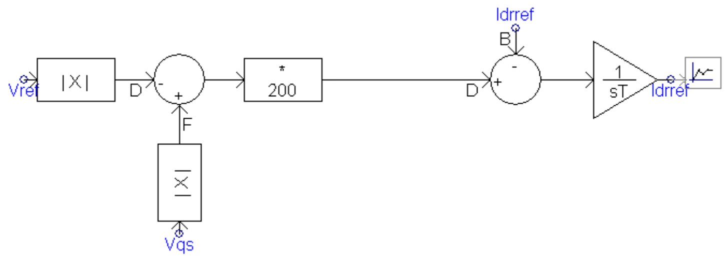

a) Primary stage

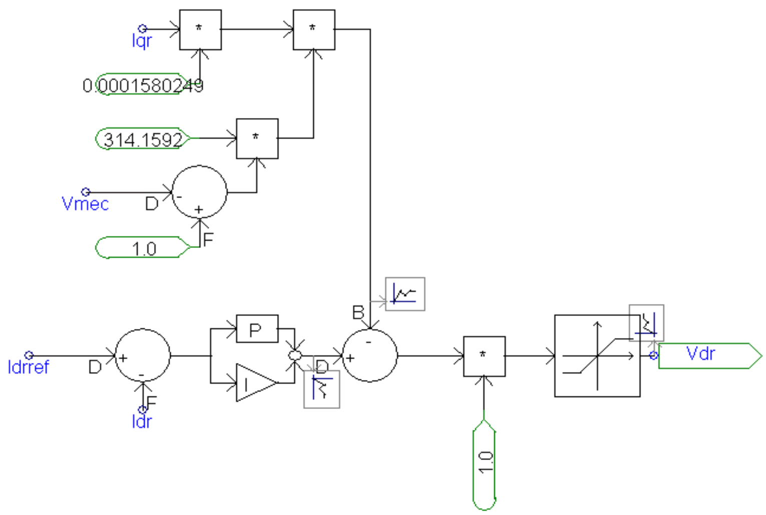

b) Secondary stage

Fig. 5 Voltage control scheme based on vector control

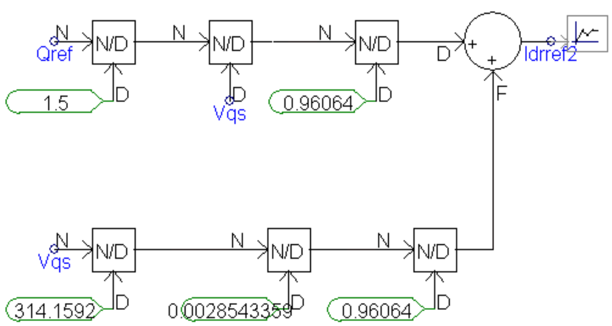

Fig. 6 Reactive power control scheme: primary stage

Substituting for ids into (25) will result in:

$$Q_s = \frac{L_m |V_s|}{(L_{ls} + L_m)} i_{dr} - \frac{|V_s|^2}{\omega_s (L_{ls} + L_m)} \qquad (26)$$

DFIG generators can be controlled in constant voltage state or in constant reactive power.

4.2 Voltage Control

In order to control terminal voltage, the amplitude of i_{dr} is controlled. In order that control voltage, reference voltage is compared with the terminal voltage. Then error control signal is produced to an integral controller, as shown in Fig. 5(a).

The secondary stage of the controller is constructed using the primary stage reference current compared to the direct component of measured rotor current. The required rotor voltage is obtained from a PI controller and the summation of the quadrature rotor current compensation term, derived from (15). This control scheme is shown in Fig. 5(b).

4.3 Reactive Power Control

For controlling reactive power, i_{drref} is obtained from (26). Its control scheme is shown in Fig. 6. The secondary stage for controlling reactive power is similar to Fig. 5(b).

5. VOLTAGE PROFILE

To illustrate the impact of a wind turbine on the voltage profile along a line, a distribution grid is considered (Figure 7) [6]. The node 1 is connected to the high voltage grid. The rated voltage is 15 kV. On average, the X/R ratio of the distribution lines in the studied grid is approximately 7.5. The total load is 10 MVA.

A wind turbine is assumed to be connected to node 9. Fig.8 shows the wind speed at hub height, used as input for the simulation.

Three cases for the turbine type are considered in the following scenarios (Table 1).

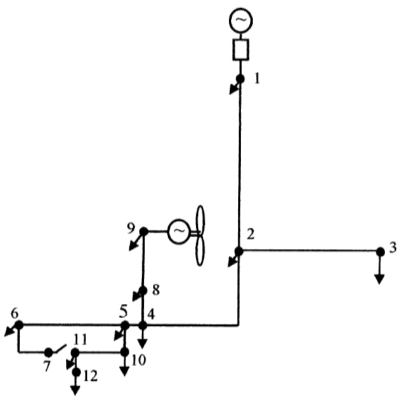

Fig. 7 Simplified one-line diagram of the study case feeder

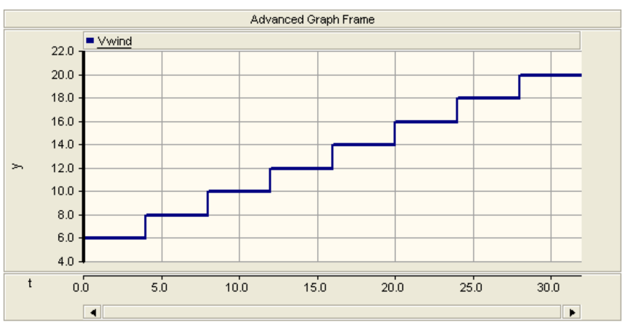

Fig. 8 Assumed wind speed, as input for the simulation

Table 1. Cases considered for simulations

	Speed controller	Generator type	Reactive power control
Case 1	fixed speed	SCIG	no
Case 2	variable speed	DFIG	cos ϕ = 1
Case 3	variable speed	DFIG	voltage control

All the generators are used in wind turbines is categorized in one of the above cases. Voltages of two nodes are shown in Fig. 9. As can be seen in the figure, the distributed generator has impact on the voltage profile along the line. The reactive power output of a SCIG (cases 1) cannot be controlled. The reactive power output is always negative (inductive behavior). In this case, reduction of voltage level is seen in Fig. 9.

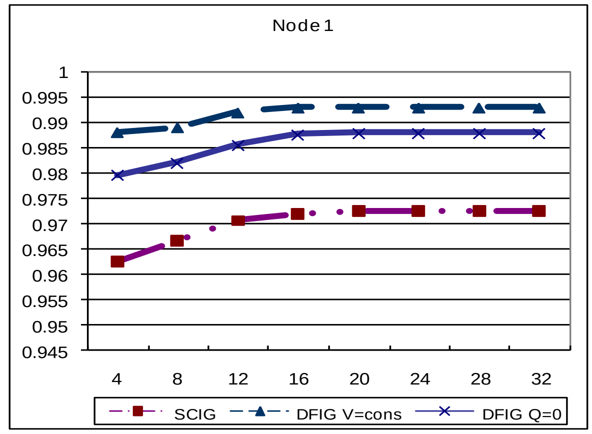

a) Voltage of node 1

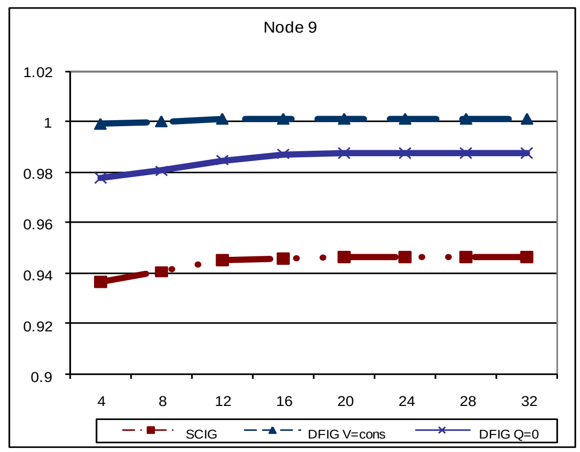

b) Voltage of node 9

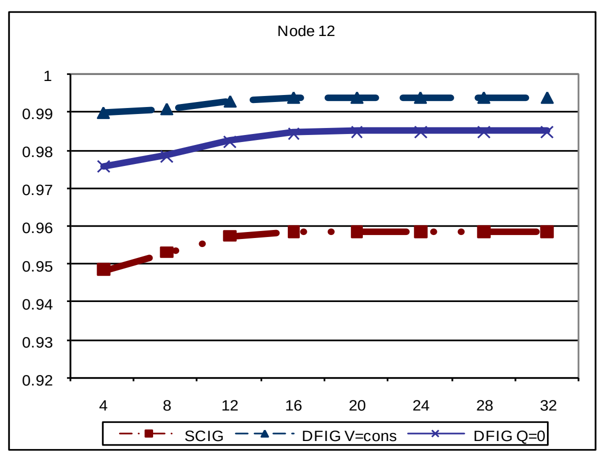

c) Voltage of node 12

Fig. 9. Voltages of some nodes

The reactive power for case 2 is permanently controlled to zero. It is seen that in case 2, voltage levels are upper than case 1. In case 3 that the DFIG is controlled in constant voltage state, the voltage in node 9 has been constant in 1 p.u in all wind speeds

The highest impact on the voltage is for this example seen at node 9, where the difference between the voltages for the case 1 and 3 is approximately 6.23%.

Also, the lowest impact (2.55%) on the voltage is at node 1, where distribution grid is connected to high voltage grid.

6. CONCLUSIONS

Each type of wind turbines has different impact on steady state voltage of distribution grids. For evaluation of these impacts, SCIG generator has been simulated that works in constant-speed operation and DFIG generator that is used in a variable-speed turbine. DFIG generator can be controlled in two ways that mentioned before: constant voltage and constant reactive power. PSCAD/EMTDC is used for simulation to investigate the impact of these turbines on a distribution grid.

In inclusion, in weak grids, voltage controlled turbines had best improvement in the voltage profile of distribution system. After that, the turbine that was controlled in constant power coefficient had better impact on the voltage profile than SCIG generator.

REFERENCES

[1] Chen, S.Z., et al., Integral Sliding-Mode Direct Torque Control of Doubly-Fed Induction Generators Under Unbalanced Grid Voltage. IEEE TRANSACTIONS ON ENERGY CONVERSION JUNE 2010. **25**(2).

[2] Foster, S., L. Xu, and B. Fox, Coordinated reactive power control for facilitating fault ride through of doubly fed induction generator- and fixed speed induction generator-based wind farms. IET Renewable Power Generation, 2010. **4**(2): p. 128-138.

[3] Zhi, D., L. Xu, and B.W. Williams, Model-Based Predictive Direct Power Control of Doubly Fed Induction Generators. IEEE TRANSACTIONS ON POWER ELECTRONICS, FEBRUARY 2010. **25**(2).

[4] Yang, L., et al., Optimal controller design of a doubly-fed induction generator wind turbine system for small signal stability enhancement. IET Generation, Transmission & Distribution, 2010. **4**(5): p. 579-597.

[5] Slootweg, J.G., et al., General model for representing variable speed wind turbines in power system dynamics simulations. IEEE Transactions on Power Systems, 2003. **18**(1): p. 144-151

[6] Boulaxis, N.G., S.A. Papathanassiou, and M.P. Papadopoulos, Wind Turbine Effect on The Voltage Profile of Distribution Networks. Renewable Energy, 2002.

[7] Muljadi, E. and C.P. Butterfield, Pitch-controlled variable-speed wind turbine generation. IEEE Transactions on Industry Applications, Jan/Feb 2001. **37**(1): p. 240-246.

[8] Kabouris, J. and F.D. Kanellos, Impacts of Large-Scale Wind Penetration on Designing and Operation of Electric Power Systems. IEEE TRANSACTIONS ON SUSTAINABLE ENERGY, JULY 2010. **1**(2).

[9] Kim, S.-K. and E.-S. Kim, PSCAD/EMTDC-Based Modeling and Analysis of a Gearless Variable Speed Wind Turbine IEEE Transactions on Energy Conversion, June 2007. **22**(2): p. 421-430.

[10] Abad, G., et al., Direct Power Control of Doubly-Fed-Induction-Generator-Based Wind Turbines Under Unbalanced Grid Voltage. IEEE TRANSACTIONS ON POWER ELECTRONICS, FEBRUARY 2010. **25**(2).

[11] Abedini, A. and H. Nikkhajoei, Dynamic model and control of a wind-turbine generator with energy storage. IET Renewable Power Generation, 2011. **5**(1).

[12] Chien-Hung , L. and H. Yuan-Yih Effect of Rotor Excitation Voltage on Steady-State Stability and Maximum Output Power of a Doubly-Fed Induction Generator. IEEE Transactions on Industrial Electronics, April 2011. **58**(4): p. 1096 - 1109

[13] Li, P., P.-K. Keung, and B.-T. Ooi, Development and simulation of dynamic control strategies for wind farms. Published in IET Renewable Power Generation, 2009. **3**(2): p. 180–189.

[14] Fan, L., et al., Modeling of DFIG-Based Wind Farms for SSR Analysis. IEEE TRANSACTIONS ON POWER DELIVERY, OCTOBER 2010. **25**(4).

[15] Rahimi, M. and M. Parniani, Transient Performance Improvement of Wind Turbines With Doubly Fed Induction Generators Using Nonlinear Control Strategy. IEEE TRANSACTIONS ON ENERGY CONVERSION, JUNE 2010. **25**(2).

[16] Luna, A., et al., Simplified Modeling of a DFIG for Transient Studies in Wind Power Applications. IEEE TRANSACTIONS ON INDUSTRIAL ELECTRONICS, JANUARY 2011. **58**(1).

[17] Li, S. and S. Sinha, A Simulation Analysis of Double-Fed Induction Generators for Wind Energy Conversion Using PSpice. IEEE Transaction on Energy Conversion Systems, 2006. **32**.

[18] M. Tazil, V.K., R.C. Bansal, S. Kong, Z.Y. Dong, W. Freitas, H.D. Mathur, Three-phase doubly fed induction generators: an overview. IET Electric Power Applications, 2010. **4**(2): p. 75–89.